Enhanced Stability and Sustained Delivery of Structurally Dense DNA Nanostructures *via* a Biodegradable Hydrogel Platform

Youngjin Choi[1,†], *Yeonju Song*[2,3,†], *Bo Kyung Cho*[1], *Sang Jin Baek*[1,4], *Jin Myeong Wang*[1], *Su Hyun Seok*[5,6,7], *William M. Shih*[5,6,7], *Junsang Doh*[3,*], *Youngmee Jung*[2,8,*], *Ju Hee Ryu*[1,4,*]

[1]Medicinal Materials Research Center, Biomedical Research Institute, Korea Institute of Science and Technology (KIST), Seoul, Republic of Korea

[2]Biomaterials Research Center, Biomedical Research Institute, KIST, Seoul, Republic of Korea

[3]Department of Materials Science and Engineering, Seoul National University, 1 Gwanak-ro, Gwanak-gu, Seoul, Republic of Korea.

[4]KU-KIST Graduate School of Converging Science and Technology, Korea University, Seoul, Republic of Korea

[5]Department of Cancer Biology, Dana-Farber Cancer Institute, Harvard Medical School, Boston, MA, USA

[6]Wyss Institute for Biologically Inspired Engineering at Harvard University, Boston, MA, USA

[7]Department of Biological Chemistry and Molecular Pharmacology, Harvard Medical School, Boston, MA, USA

[8]School of Electrical and Electronic Engineering, YU-KIST Institute, Yonsei University, Seoul, Republic of Korea

[†]These authors contributed equally to this work

[*]Corresponding authors: jsdoh@snu.ac.kr (J.D.); winnie97@kist.re.kr (Y.J.); jhryu@kist.re.kr (J.H.R.)

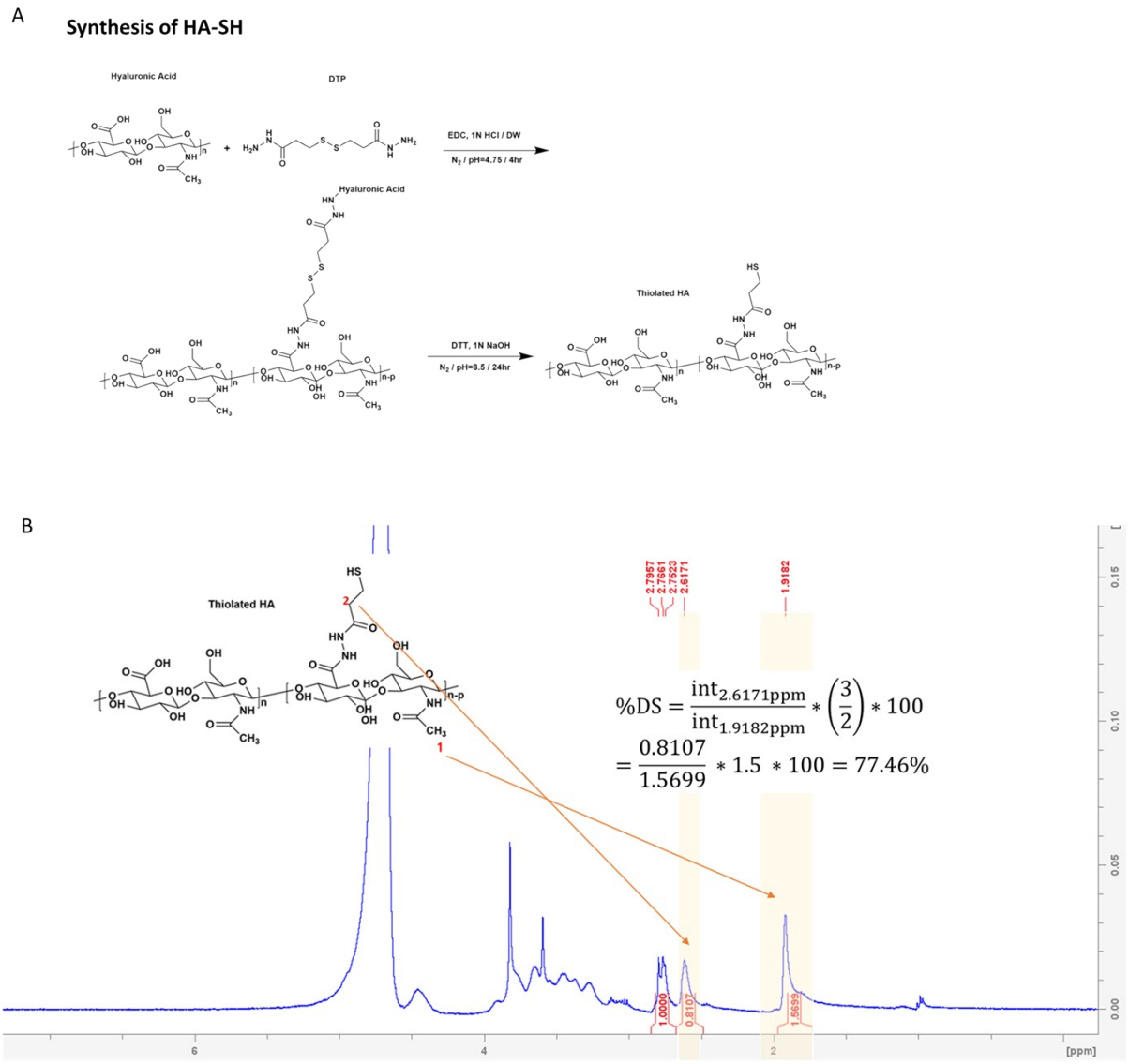

Figure S1. Synthesis and characterization of HA-SH. (A) Schematic illustration of the HA-SH synthesis scheme. H-NMR spectrum confirming the successful substitution of thiol groups onto the hyaluronic acid backbone. The degree of substitution (DS) was calculated to be 77.46%, and this synthesized batch was used for all subsequent experiments.

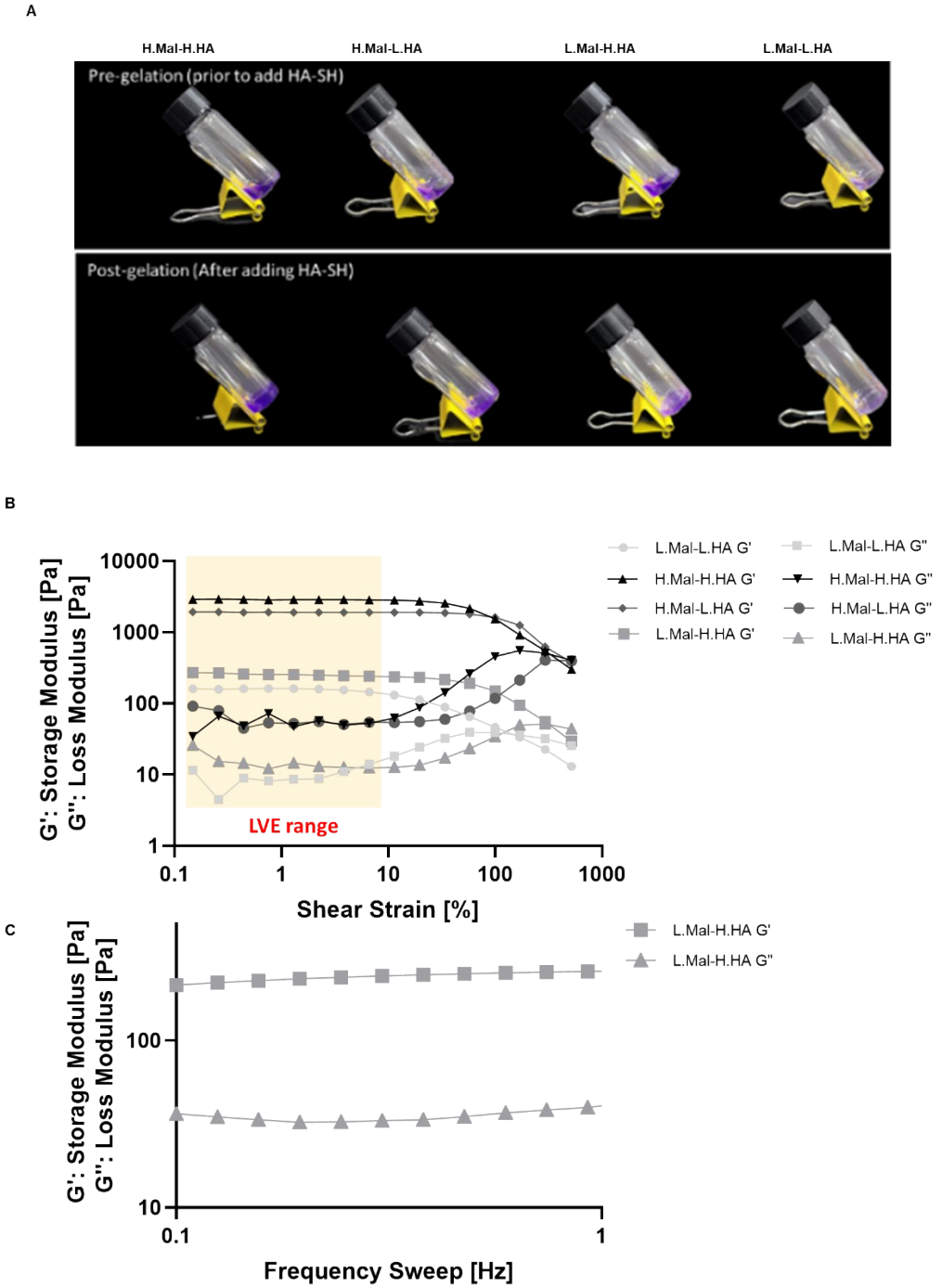

Figure S2. (A) Images of four differently formulated hydrogels pre- and post-gelation. Gelation is confirmed by the side-view images on an inclined surface. Post-gelation hydrogels at all four formulations confirm complete and homogeneous gelation of the hydrogel. (B) Amplitude sweep analysis of four HA/gelatin hydrogel formulations (H.Mal-H.HA, H.Mal-L.HA, L.Mal-H.HA, L.Mal-L.HA). Storage modulus (G′) and loss modulus (G″) were measured across 0.1–100 % strain at a fixed frequency of 1 Hz. The shaded region denotes the linear viscoelastic (LVE) range used for subsequent mechanical characterization. (C) Frequency sweep analysis of a representative L.Mal-H.HA hydrogel conducted within the LVE regime (1% strain), measuring G′ and G″ over a frequency range of 0.1—1 Hz. The data demonstrate formulation-dependent differences in network stiffness and viscoelastic behavior.

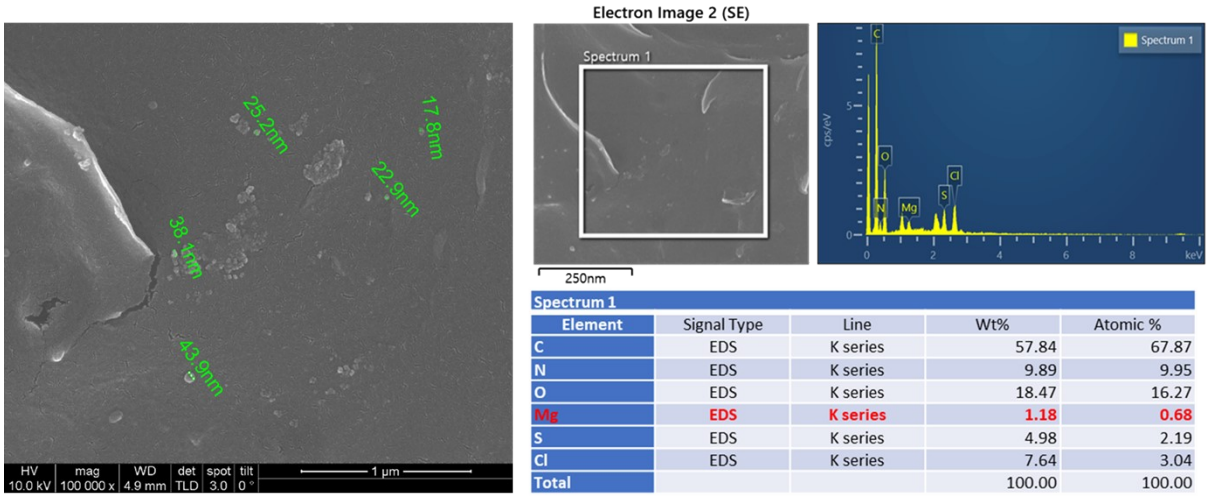

Spectrum 1

Element	Signal Type	Line	Wt%	Atomic %
C	EDS	K series	57.84	67.87
N	EDS	K series	9.89	9.95
O	EDS	K series	18.47	16.27
Mg	EDS	K series	1.18	0.68
S	EDS	K series	4.98	2.19
Cl	EDS	K series	7.64	3.04
Total			100.00	100.00

Figure S3. SEM and EDS analyses of the HA/gelatin hydrogel showing the presence of Mg^{2+} ions within the network.

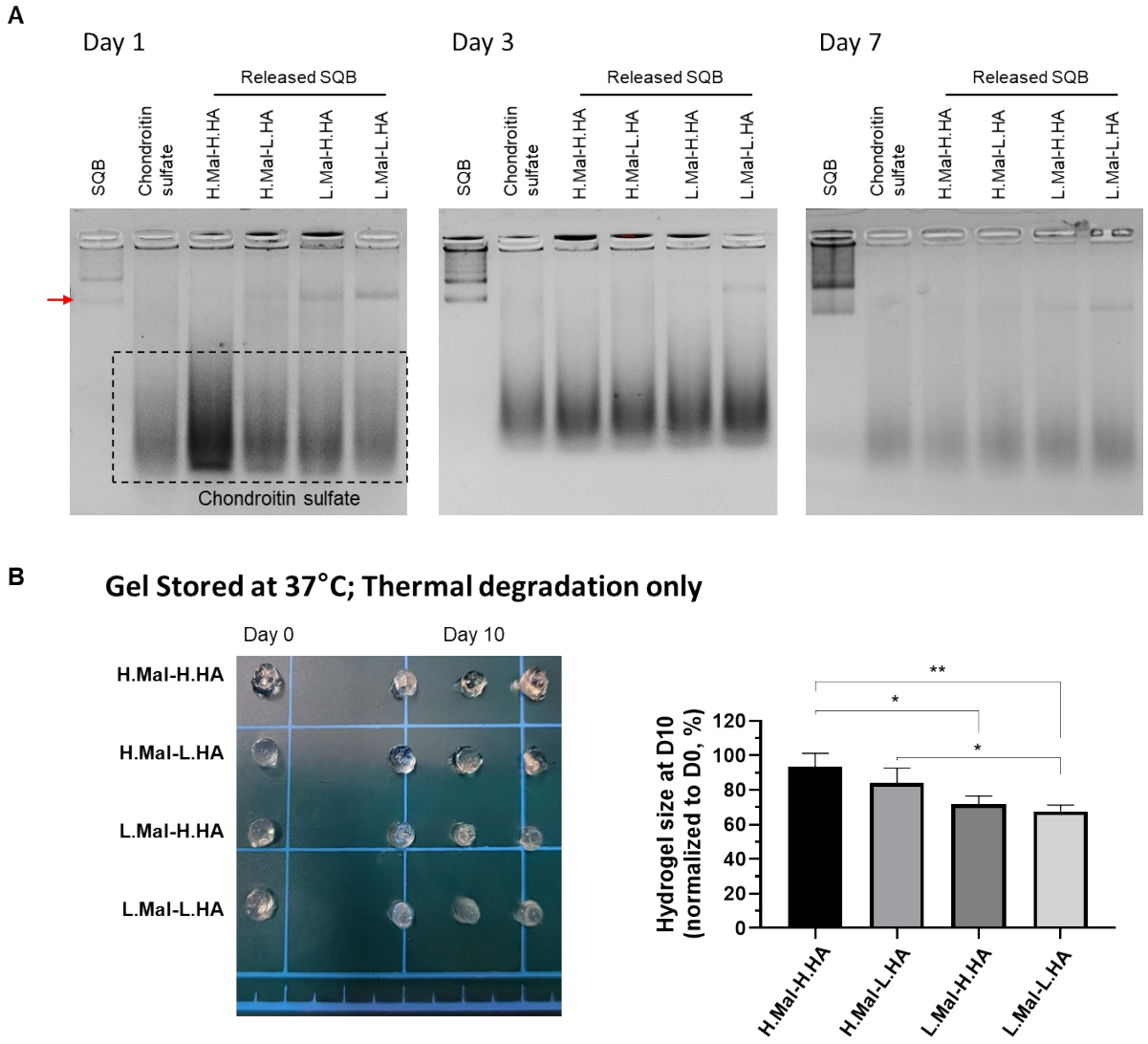

Figure S4. (A) Agarose gel electrophoresis of SQBs released into PBS analyzed at day 1, 3, and 7 (37 ℃, no enzyme). The pristine SQB control exhibits a distinct, single band (red arrow), confirming structural integrity. Notably, the loosely crosslinked groups (L.Mal-H.HA and L.Mal-L.HA) display more prominent band intensities compared to denser formulations. This visually corroborates the higher release profile driven by thermal gelatin softening and restricted diffusion mechanisms shown in **Figure 3B**. Chondroitin sulfate used for K_{10}-PEG layer removal may contribute to the background signal in the lower region (black dashed box). (B) Bright-field images of hydrogel samples after 10-day incubation in PBS at 37 ℃. Hydrogels with lower crosslinking density exhibited more prominent shrinkage, while highly crosslinked hydrogels retained their original volume and morphology. Quantification of hydrogel degradation based on residual volume analysis using bright-field images of hydrogel samples. H.Mal–H.HA hydrogel retained 93.7% of its original volume, whereas L.Mal–L.HA retained 67.7%, reflecting differences in crosslinking density and gelatin content. Data represent mean ± SD (n = 3). Statistical significance was evaluated using one-way ANOVA followed by Tukey's post hoc test (*$p < 0.05$, **$p < 0.01$).

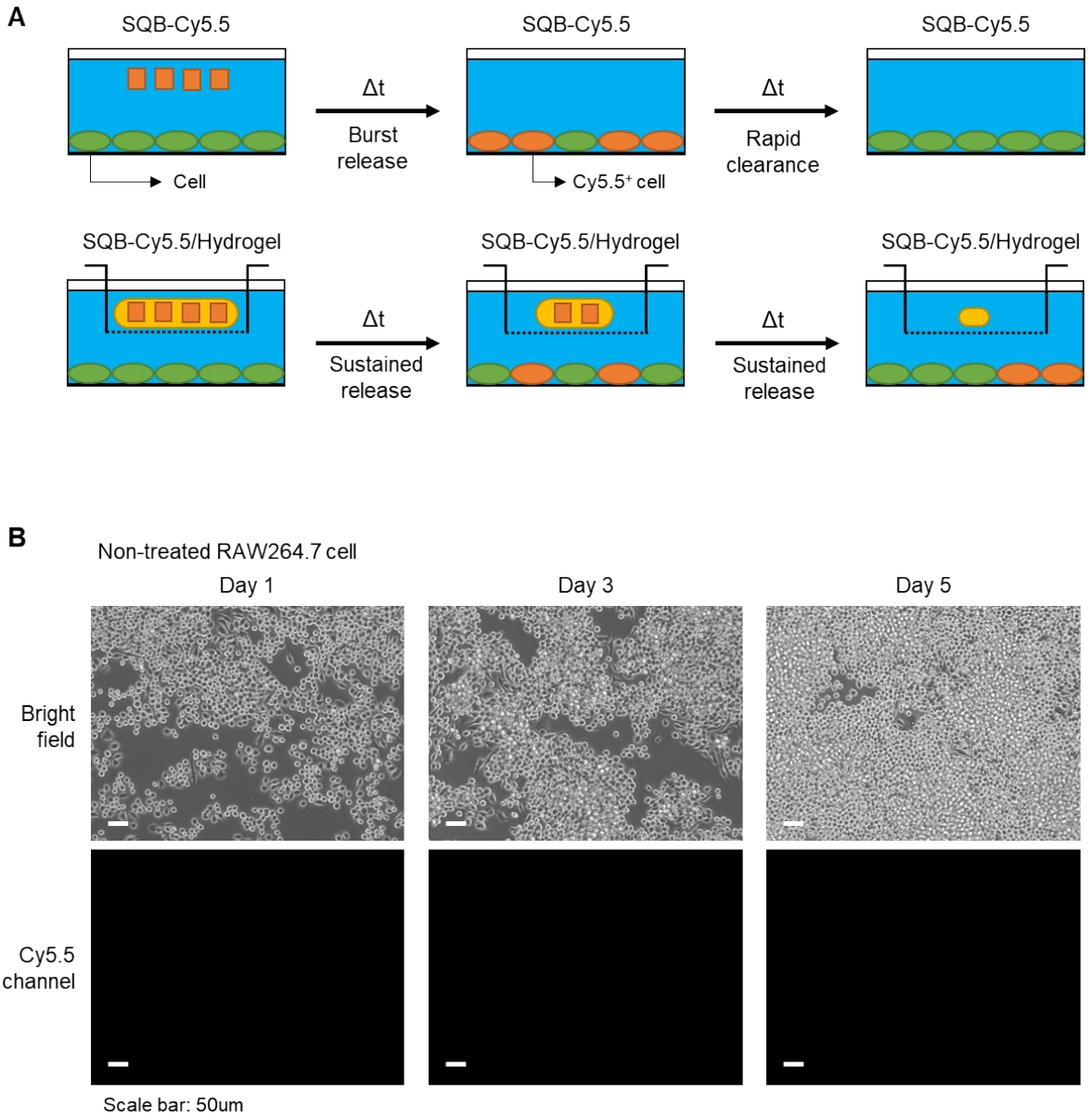

Figure S5. (A) Schematic illustration of the experimental setup used to compare cellular exposure to free SQBs versus hydrogel-mediated release. For the free SQB condition, Cy5.5-labeled SQBs were added directly to the culture well, resulting in immediate contact and rapid cellular uptake. For the hydrogel condition, SQB–hydrogel hybrids were placed in the upper chamber of a Transwell insert, allowing SQBs to reach cells only through diffusion-mediated release across the membrane. This configuration enables temporal separation between burst uptake (free SQBs) and sustained, gradual uptake (hydrogel-released SQBs). (B) Representative bright-field and Cy5.5 fluorescence images of non-treated RAW 264.7 macrophages used as negative controls.

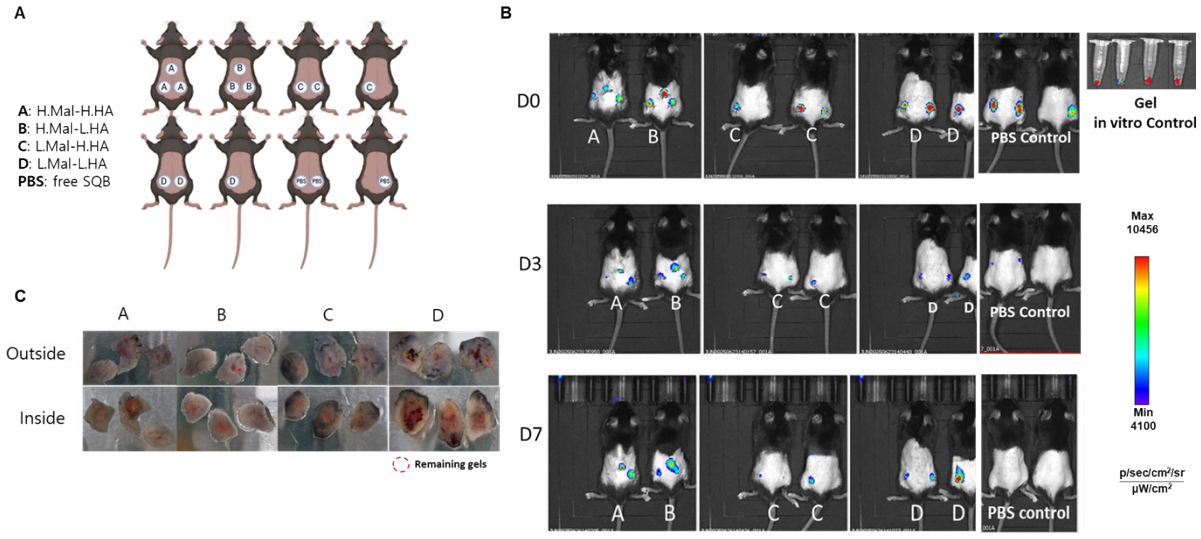

Figure S6. (A) Illustration of the dorsal implantation sites for SQB–hydrogel hybrids and free SQB injections. (B) Whole-body IVIS fluorescence images of mice at days 0, 3, and 7, showing the prolonged fluorescence retention at hydrogel sites compared to free SQB. (C) Photographs of excised tissues on day 10, confirming the presence of residual hydrogels.